Structural Engineering and Mechanics, Vol. 21, No. 6 (2005) 635-658
DOI: http://dx.doi.org/10.12989/sem.2005.21.6.635

Detection of crack in L-shaped pipes filled with fluid based on transverse natural frequencies

S. M. Murigendrappa†, S. K. Maiti‡ and H. R. Srirangarajan‡†

Mechanical Engineering Department, Indian Institute of Technology Bombay, Powai, Mumbai 400076, India

(Received December 18, 2003, Revised April 28, 2005, Accepted September 28, 2005)

Abstract. The possibility of detecting a crack in L-shaped pipes filled with fluid based on measurement of transverse natural frequencies is examined. The problem is solved by representing the crack by a massless rotational spring, simulating the out-of-plane transverse vibration only without solving the coupled torsional vibration and using the transfer matrix method for solution of the governing equation. The theoretical solutions are verified by experiments. The cracks considered are external, circumferentially oriented and have straight front. Pipes made of aluminium and mild steel are tested with water as internal fluid. Crack size to pipe thickness ratio ranging from 0.20 to 0.57 and fluid (gauge) pressure in the range of 0 to 10 atmospheres are examined. The rotational spring stiffness is obtained by an inverse vibration analysis and deflection method. The details of the two methods are given. The results by the two methods are presented graphically and show good agreement. Crack locations are also determined by the inverse analysis. The maximum absolute error in the location is 13.80%. Experimentally determined variation of rotational spring stiffness with ratio of crack size to thickness is utilized to predict the crack sizes. The maximum absolute errors in prediction of crack size are 17.24% and 16.90% for aluminium and mild steel pipes respectively.

Key words: detection of crack; out-of-plane transverse vibration; L-shaped pipe filled with fluid; transfer matrix method; rotational spring.

1. Introduction

Long pipes abundantly occur in power plants, chemical plants, and oil and natural gas industries. They are used to transport fluid at different pressures. Most often the pipes are employed in long spans. Monitoring health of such pipes in service is very important for ensuring an uninterrupted operation. Health can be monitored using non-destructive testing techniques, e.g., X-ray, electric impedance technique, eddy current based method, etc. These methods require scanning of the whole length of a pipe. This process is a very time consuming, labour-intensive and expensive. One emerging potential candidate for the detection is based on changes in vibration responses of a component. Its usefulness has been shown (Wauer 1990, Gasch 1993, Dimarogonas 1996, Salawu

† Ex-Research Scholar
‡ Professor, Corresponding author, E-mail: skmaiti@me.iitb.ac.in
‡† Professor

1997, Doebling *et al.* 1998) to a laboratory scale for components in the form of beams. The method makes use of either the global or local effects produced by a crack. The changes in natural frequencies form the basis of one of such global methods. This has suitability for components with limited or full access. The limited access is common for pipes located in hazardous areas of nuclear power plants and under-sea pipelines. The changes in displacements and mode shapes (or its derivatives like strains, and curvatures) are the basis of the local methods, which are appropriate for components with full access. The method based on natural frequencies is more attractive because the frequency can be measured easily from any point on the component. Its applicability has been shown for beams with external cracks, normal or inclined at an angle to the edge, single and multiple cracks (e.g., Hu and Liang 1993, Nandwana and Maiti 1997, Li 2002, Ruotolo and Surace 1997). The method does not involve any iteration and is alright for any component whose free vibrations can be modelled in a particular manner with and without crack. For straight beams the focus has been more on free transverse vibrations than axial and torsional vibrations. The method based on the transverse vibration is of interest here.

While modelling, the governing equations are obtained through the Euler-Bernoulli beam theory for long beams and the Timoshenko theory for short beams. The local effects of a crack are represented either in the form of a segment of reduced section height symmetrically placed around it (Bovsunovsky and Matveev 2000) or by a rotational spring (Hu and Liang 1993, Nandwana and Maiti 1997, Li 2002, Liang *et al.* 1991, Murigendrappa *et al.* 2004, Patil and Maiti 2002, Choy *et al.* 1995, Chaudhari and Maiti 2000, Chaudhari 2000) invoked at the crack location. The approach based on the rotational spring assumes that a crack alters the mode shape of the beam only locally. The rotational spring stiffness corresponding to a given crack can be determined from the relationship between the stress intensity factor and the crack size. In the absence of such a relationship it can be determined experimentally or numerically through the displacement method or inverse vibration analysis (e.g., Hu and Liang 1993, Nandwana and Maiti 1997, Chaudhari and Maiti 2000, Murigendrappa *et al.* 2004). In the displacement method, the relationship between the rotational spring stiffness and the difference in strain energies of a beam corresponding to two configurations, with and without crack, and the same loading, is utilized to determine the stiffness.

A wide variety of beams have been considered for crack detection, e.g., beams with uniform section, discretely or continuously varying section, only supported at the ends on rigid or elastic supports, intermittently supported on rigid or elastic supports (Liang *et al.* 1991, Narkis 1994, Choy *et al.* 1995, Nandwana and Maiti 1997, Chaudhari and Maiti 2000, Patil and Maiti 2002, Kim and Stubbs 2003), etc. Experimental results, though not very exhaustive, are also reported.

Most of the studies on frames consider them to be made of prismatic bars. They address the forward problem of determination of natural frequencies knowing the crack details (e.g., Chondros and Dimarogonas 1989, Saavedra and Cuitiño 2001) and inverse problem of determination of crack details from the natural frequencies (e.g., Yao *et al.* 1992, Hassiotis and Jeong 1993, Morassi and Rovere 1997, Nikolakopoulos *et al.* 1997, Shi *et al.* 1998, Hassiotis 1999, Xia and Hao 2000). Pipes filled with fluid under pressure have not yet been studied. Pipes can occur in straight or framed configurations. The simplest framed pipe is in the form of L. In the case of such pipes, there is a possibility of cracks developing in service at the internal surface due to stress-corrosion. There is also a possibility of cracks developing at the external surface in circumferential orientation due to the dominance of mechanical loading and/or stress-corrosion. Both the problems have practical importance; the external crack is of concern here. Some of the studies (e.g., Chaudhari 2000) show the possibility of detection of crack in straight empty pipes. A field pipe, which may contain fluid,

is therefore required to be emptied, detached and taken to the laboratory for the vibration-based crack detection. To help attain an in-situ testing capability they should be tested in the laboratory under conditions similar to the operating conditions. Murigendrappa *et al.* (2004) present an attempt in this direction for straight pipes.

Leak-before-break is an established concept for pipelines carrying fluids under pressure. This has motivated many on-line monitoring schemes and detection of leak-before-break for pipelines. If the crack can be detected before it gives way to leaking, it will have a lot of practical utility. This is also an important motivating factor for the present study.

In the case of free transverse vibration of L-shaped pipes with two orthogonal segments, particularly in the case of out-of-plane vibrations, there is a coupling of bending and torsional effects. For such pipes without any crack, Murigendrappa (2004) has proposed an approach of modelling by considering only transverse vibration of each segment separately without solving the coupled torsional vibration. In the approach, the coupling of torsional and transverse vibrations have been decoupled by an inclusion of total torsional effect due to one segment on the transverse vibration of the other in a way which is akin to lumping.

This paper presents an extension of the method of vibration analysis for crack-free L pipes proposed by Murigendrappa (2004) to similar pipes with a crack and gives a procedure for detection of single crack in such pipes. The problem has been solved by combining the massless rotational spring based representation of a crack and the transfer matrix method for solution of the governing equation. The cracks considered are external, normal to the axis and have straight front part through-the-thickness, i.e., a non-leaking crack. The rotational spring stiffness has been measured experimentally by the displacement method and the inverse vibration analysis knowing the changes in natural frequencies. Experimental studies are presented to demonstrate the effectiveness of the method for the prediction of rotational spring stiffness, crack location and its size through the measurement of natural frequencies.

2. Theoretical formulation

For an L-shaped pipe without any crack filled with an incompressible fluid, neglecting effects of shear deformation, rotational inertia and damping, the free out-of-plane transverse motion of each segment is governed by (Fig. 1a)

$$EI\frac{\partial^4 y_i}{\partial x_i^4} + pA_{fp}\frac{\partial^2 y_i}{\partial x_i^2} + [\rho_P A_P + \rho_f A_{fp}]\frac{\partial^2 y_i}{\partial t^2} = 0 \tag{1}$$

where E is the modulus of elasticity, I is the second moment of inertia, ρ_P is the density of material of pipe, ρ_f is the density of fluid, A_{fp} and A_P are cross sectional area of fluid cylinder and pipe respectively, p is fluid pressure, y_i is the transverse displacement of the pipe as a function of position x_i along the length of the pipe in a particular mode for the segment i. Considering harmonic motion and

$$y_i(\eta_i, t) = v_i(\eta_i)\sin(\omega t) \tag{2}$$

where $\eta_i = x_i/L_i$ for ith segment, the mode shape equation is obtained.

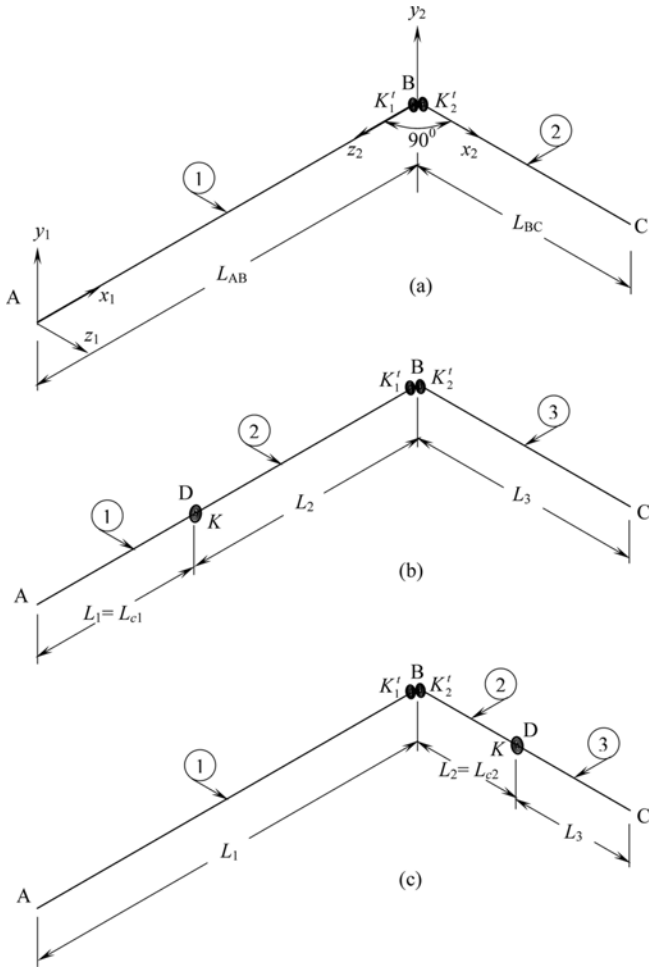

Fig. 1 L-shaped pipe. (a) Crack-free. Crack is represented by rotational spring at D in (b) segment AB and (c) segment BC

$$\frac{\partial^4 v_i}{\partial \eta_i^4} + \frac{A_{fp} p L_i^2}{EI} \frac{\partial^2 v_i}{\partial \eta_i^2} - \frac{\omega^2 L_i^4 [\rho_P A_P + \rho_f A_{fp}]}{EI} v_i = 0 \tag{3}$$

The solution of Eq. (3) is given by

$$v_i(\eta_i) = A_i \sinh(\lambda_{1,i}\ \eta_i) + B_i \cosh(\lambda_{1,i}\ \eta_i) + C_i \sin(\lambda_{2,i}\ \eta_i) + D_i \cos(\lambda_{2,i}\ \eta_i) \tag{4}$$

where $\lambda_{1,i} = \phi_1 L_i$, $\lambda_{2,i} = \phi_2 L_i$ for ith segment and

$$\left.\begin{matrix}\phi_1 \\ \phi_2\end{matrix}\right\} = \frac{\left[\mp \frac{A_{fp} p}{EI} + \left\{\left(\frac{A_{fp} p}{EI}\right)^2 + \frac{4\omega^2 [\rho_P A_P + \rho_f A_{fp}]}{EI}\right\}^{1/2}\right]^{1/2}}{2}$$

A_i, B_i, C_i and D_i are arbitrary constants determined from the boundary conditions.

For a similar pipe with a crack, the segment with crack is split into two parts, which are connected by a rotational spring of stiffness K at the crack location D (Figs. 1b or c). The governing equation of motion of AD, DB and BC (Fig. 1b) or AB, BD and CD (Fig. 1c) is of the type of Eq. (1). The transfer matrix method for each segment can be easily obtained using Eq. (4). The state vectors $\{\boldsymbol{v}\}_C$ associated with the end C (Figs. 1b or c), can be written in terms of $\{\boldsymbol{v}\}_A$ of the end A, as follows.

Case 1 (Fig. 1b):

$$\{\boldsymbol{v}\}_C = [\mathbf{T}]_3[\mathbf{T}^t]_2[\mathbf{T}]_J[\mathbf{T}^t]_1[\mathbf{T}]_2[\mathbf{T}]_K[\mathbf{T}]_1\{\boldsymbol{v}\}_A \tag{5}$$

Case 2 (Fig. 1c):

$$\{\boldsymbol{v}\}_C = [\mathbf{T}]_3[\mathbf{T}]_K[\mathbf{T}]_2[\mathbf{T}^t]_2[\mathbf{T}]_J[\mathbf{T}^t]_1[\mathbf{T}]_1\{\boldsymbol{v}\}_A \tag{6}$$

where $\{\boldsymbol{v}\}= \{v\ \theta\ M\ V\ M_t\ \theta_t\}^T$ and $[\mathbf{T}]_i$ is the matrix of ith segment. $[\mathbf{T}^t]_1$ and $[\mathbf{T}^t]_2$ are the matrices linking the two sides of the torsional springs located at B. $[\mathbf{T}]_J$ links the state variables associated with the ends of the two segments AB and BC, and $[\mathbf{T}]_K$ is the transfer matrix for the crack. These matrices are given below.

$$[\mathbf{T}]_i = \begin{bmatrix} T_{11}^{(i)} & T_{12}^{(i)} & T_{13}^{(i)} & T_{14}^{(i)} & 0 & 0 \\ T_{21}^{(i)} & T_{22}^{(i)} & T_{23}^{(i)} & T_{24}^{(i)} & 0 & 0 \\ T_{31}^{(i)} & T_{32}^{(i)} & T_{33}^{(i)} & T_{34}^{(i)} & 0 & 0 \\ T_{41}^{(i)} & T_{42}^{(i)} & T_{43}^{(i)} & T_{44}^{(i)} & 0 & 0 \\ 0 & 0 & 0 & 0 & -1 & 0 \\ 0 & 0 & 0 & 0 & \dfrac{1}{K_i^t} & 1 \end{bmatrix}, \quad [\mathbf{T}]_K = \begin{bmatrix} 1 & 0 & 0 & 0 & 0 & 0 \\ 0 & 1 & \dfrac{1}{K} & 0 & 0 & 0 \\ 0 & 0 & 1 & 0 & 0 & 0 \\ 0 & 0 & 0 & 1 & 0 & 0 \\ 0 & 0 & 0 & 0 & 1 & 0 \\ 0 & 0 & 0 & 0 & 0 & 1 \end{bmatrix}$$

$$[\mathbf{T}]_J = \begin{bmatrix} 1 & 0 & 0 & 0 & 0 & 0 \\ 0 & 0 & 0 & 0 & 0 & 1 \\ 0 & 0 & 0 & 0 & 1 & 0 \\ 0 & 0 & 0 & 1 & 0 & 0 \\ 0 & 0 & 1 & 0 & 0 & 0 \\ 0 & 1 & 0 & 0 & 0 & 0 \end{bmatrix}, \quad [\mathbf{T}^t]_1 = \begin{bmatrix} 1 & 0 & 0 & 0 & 0 & 0 \\ 0 & 1 & \dfrac{1}{K_1^t} & 0 & 0 & 0 \\ 0 & 0 & 1 & 0 & 0 & 0 \\ 0 & 0 & 0 & 1 & 0 & 0 \\ 0 & 0 & 0 & 0 & 1 & 0 \\ 0 & 0 & 0 & 0 & 0 & 1 \end{bmatrix}$$

$$[\mathbf{T}^t]_2 = \begin{bmatrix} 1 & 0 & 0 & 0 & 0 & 0 \\ 0 & 1 & \dfrac{1}{K_2^t} & 0 & 0 & 0 \\ 0 & 0 & 1 & 0 & 0 & 0 \\ 0 & 0 & 0 & 1 & 0 & 0 \\ 0 & 0 & 0 & 0 & 1 & 0 \\ 0 & 0 & 0 & 0 & 0 & 1 \end{bmatrix}$$

where $i = 1, 2$ and 3, $T_{11}^{(i)} = \dfrac{\Theta_i^2 \cosh\Omega_i + \Omega_i^2 \cos\Theta_i}{\Gamma_i}$, $T_{12}^{(i)} = \dfrac{L_i}{\Gamma_i}\left(\dfrac{\Theta_i^2 \sinh\Omega_i}{\Omega_i} + \dfrac{\Omega_i^2 \sin\Theta_i}{\Theta_i}\right)$

$$T_{13}^{(i)} = \frac{L_i^2[\cosh\Omega_i - \cos\Theta_i]}{EI\Gamma_i},\quad T_{14}^{(i)} = \frac{L_i^3}{EI\Gamma_i}\left(\frac{\sinh\Omega_i}{\Omega_i} - \frac{\sin\Theta_i}{\Theta_i}\right),\quad T_{21}^{(i)} = \frac{\Omega_i\Theta_i^2\sinh\Omega_i - \Omega_i^2\Theta_i\sin\Theta_i}{L_i\Gamma_i}$$

$$T_{22}^{(i)} = \frac{\Theta_i^2\cosh\Omega_i + \Omega_i^2\cos\Theta_i}{\Gamma_i},\quad T_{23}^{(i)} = \frac{L_i[\Omega_i\sinh\Omega_i + \Theta_i\sin\Theta_i]}{EI\Gamma_i},\quad T_{24}^{(i)} = \frac{L_i^2[\cosh\Omega_i - \cos\Theta_i]}{EI\Gamma_i}$$

$$T_{31}^{(i)} = \frac{EI\Lambda_i[\cosh\Omega_i - \cos\Theta_i]}{L_i^2\Gamma_i},\quad T_{32}^{(i)} = \frac{EI[\Omega_i\Theta_i^2\sinh\Omega_i - \Omega_i^2\Theta_i\sin\Theta_i]}{L_i\Gamma_i}$$

$$T_{33}^{(i)} = \frac{\Omega_i^2\cosh\Omega_i + \Theta_i^2\cos\Theta_i}{\Gamma_i},\quad T_{34}^{(i)} = \frac{L_i[\Omega_i\sinh\Omega_i + \Theta_i\sin\Theta_i]}{\Gamma_i}$$

$$T_{41}^{(i)} = \frac{EI\Lambda_i[\Omega_i\sinh\Omega_i + \Theta_i\sin\Theta_i]}{L_i^3\Gamma_i},\quad T_{42}^{(i)} = \frac{EI\Lambda_i[\cosh\Omega_i - \cos\Theta_i]}{L_i^2\Gamma_i},\quad T_{43}^{(i)} = \frac{\Omega_i^3\sinh\Omega_i - \Theta_i^3\sin\Theta_i}{L_i\Gamma_i}$$

$$T_{44}^{(i)} = \frac{\Omega_i^2\cosh\Omega_i + \Theta_i^2\cos\Theta_i}{\Gamma_i},\ \Omega_i = \lambda_{1,i},\ \Theta_i = \lambda_{2,i},\ \Gamma_i = \lambda_{1,i}^2 + \lambda_{2,i}^2,\ \Lambda_i = \lambda_{1,i}^2\lambda_{2,i}^2,\ \lambda_{1,i} = \phi_1 L_i$$

$\lambda_{2,i} = \phi_2 L_i$, $K_i^t = GJ/L_i$, $K_1^t = GJ/L_{\mathrm{BC}}$, $K_2^t = GJ/L_{AB}$, G and J are shear modulus of elasticity and polar moment of inertia of the pipe cross-section respectively.

The following characteristic determinant of size 3×3 is obtained after inserting the end conditions for the fixed-free pipe in Eq. (5) for the case of crack is located in segment AB.

$$\begin{vmatrix} A_{11} + \dfrac{B_{11}}{K} & A_{12} + \dfrac{B_{12}}{K} & A_{13} \\ A_{21} + \dfrac{B_{21}}{K} & A_{22} + \dfrac{B_{22}}{K} & A_{23} \\ A_{31} - \dfrac{B_{31}}{K} & A_{32} - \dfrac{B_{32}}{K} & 0 \end{vmatrix} = 0 \tag{7}$$

where A_{ij} and B_{ij} are explicitly given in Appendix I. A and C are considered fixed and free ends respectively (Fig. 1).

Alternatively, Eq. (7) can be written in the following form and it can be used to solve the inverse problem.

$$K = \frac{-A_{11}A_{23}B_{32} + A_{23}A_{32}B_{11} + A_{12}A_{23}B_{31} - A_{23}A_{31}B_{12} + A_{13}A_{21}B_{32} - A_{13}A_{32}B_{21} + A_{31}A_{13}B_{22} - A_{13}A_{22}B_{31}}{-A_{11}A_{23}A_{32} + A_{12}A_{23}A_{31} + A_{13}A_{21}A_{32} - A_{31}A_{22}A_{13}} \tag{8}$$

In the case of the crack is located in segment BC, the relations corresponding to Eqs. (7) and (8) are given below.

$$\begin{vmatrix} A_{11}+\dfrac{B_{11}}{K} & A_{12}+\dfrac{B_{12}}{K} & A_{13}+\dfrac{B_{13}}{K} \\ A_{21}+\dfrac{B_{21}}{K} & A_{22}+\dfrac{B_{22}}{K} & A_{23}+\dfrac{B_{23}}{K} \\ A_{31} & A_{32} & 0 \end{vmatrix} = 0 \tag{9}$$

and

$$K = \frac{A_{11}A_{32}B_{23}+A_{32}A_{23}B_{11}-A_{12}A_{31}B_{23}-A_{31}A_{23}B_{12}-A_{13}A_{32}B_{21}+A_{13}A_{31}B_{22}-A_{32}A_{21}B_{13}+A_{31}A_{22}B_{13}}{-A_{11}A_{32}A_{23}+A_{12}A_{23}A_{31}+A_{13}A_{21}A_{32}-A_{31}A_{22}A_{13}} \tag{10}$$

where A_{ij} and B_{ij} are explicitly given in Appendix II. Since the transfer matrices for the segments AD and DB (Fig. 1a), or BD and DC (Fig. 1c), depend on the crack location and the natural frequency, the right hand sides of Eqs. (8) and (10) are functions of the crack location and natural frequency.

3. Rotational spring stiffness

The change in strain energy of a pipe with and without a crack under the action of a constant transverse load is equal to the energy released due to the crack. That is,

$$\Delta U = \int_{A_c} \frac{K_I^2}{2E} dA = U_c - U_{nc} \tag{11}$$

where K_I is the stress intensity factor for first mode crack, U_c and U_{nc} are strain energy of the pipe with and without crack and A_c is area of crack. When the rotational spring is used to represent the crack, this energy released gets stored in the spring. This is also given by

$$\Delta U = \frac{M_{empty\ pipe}^2}{2K} \tag{12}$$

where $M_{empty\ pipe} = [P + W_P L_{BC}]L_{DB} + \dfrac{W_P L_{DB}^2}{2}$ (Fig. 2) is bending moment at the crack section due

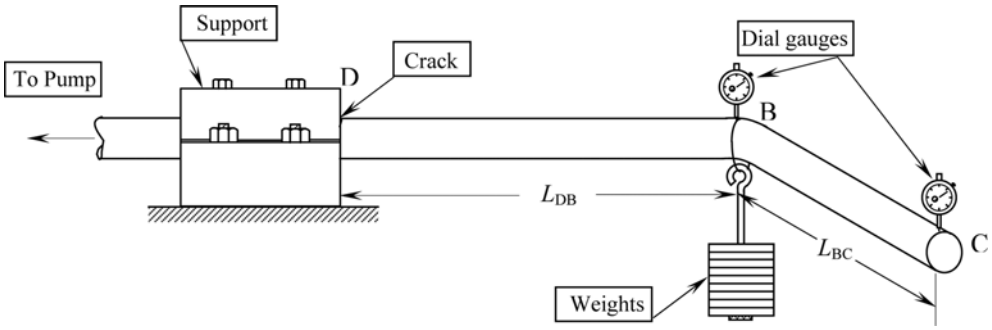

Fig. 2 Schematic representation of experimental setup for measurement of static deflection

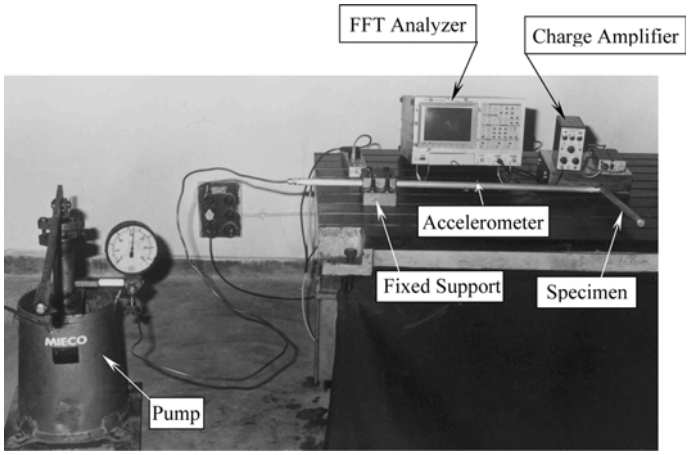

Fig. 3 Photograph of experimental setup for frequency measurement

to loading P and self weight W_P, L_{DB} is the length between the crack location and load point and K is the rotational spring stiffness. The difference ΔU can be calculated by applying a load P on the pipe and measuring the deflections in the two cases. That is,

$$\Delta U = U_c - U_{nc} = \frac{P(\delta_c - \delta_{nc})}{2} \tag{13}$$

when the pipe is empty and δ_{nc} and δ_c are the corresponding deflections along the load line. Therefore,

$$K = \frac{M^2_{empty\ pipe}}{P(\delta_c - \delta_{nc})} \tag{14}$$

For the case of a pipe with a fluid under pressure, considering the weight of fluid and pipe and its contributions to deflections, it is again possible to write

$$\Delta U = \frac{M^2_{fluid\ filled\ pipe}}{2K} \tag{15}$$

where $M_{fluid\ filled\ pipe} = [P + W_{FP}L_{\mathrm{BC}}]L_{\mathrm{DB}} + \frac{W_{FP}L^2_{\mathrm{DB}}}{2} - A_{fp}p\delta_{nc}$, W_{FP} is the total weight of the fluid and pipe material per unit length.

4. Experimental determination of rotational spring stiffness

Experiments were conducted to determine the rotational spring stiffness through both the static deflection and vibration methods. Specimens were made out of aluminium and mild steel pipes. L-shaped pipes were fabricated by welding two straight pipes AB and BC (Fig. 1) at an included angle of 90°. Before welding edges of the segments were prepared and circumferential welding

was done. Sufficient care was taken to see that the two segments were at right angle to each other. A special fixture was made to hold the two segments during the welding. Tests were conducted with empty and water filled pipes. Both pressurized and no pressure conditions were examined. Three water pressures (gauge) were considered: 0, 491 kPa and 981 kPa. All tests were carried out with cantilever conditions. Aluminium pipe details are: L_1 = 0.6 m, L_2 = 0.34 m, external diameter D_o = 0.02 m and internal diameter D_i = 0.013 m, material density ρ = 2645 kg/m^3, Young's modulus E = 60 GPa and shear modulus G = 25.5 GPa. Similar details for mild steel pipes are: L_1 = 0.6 m, L_2 = 0.3405 m, D_o = 0.019 m, D_i = 0.011 m, ρ = 7860 kg/m^3, Young's modulus E = 190 GPa and shear modulus G = 70.5 GPa. For testing under water filled conditions, one end of the pipe was closed by welding a cap. The other end was closed by a threaded stainless steel end cap, which was connected by a pipe to a hand operated hydraulic pump. To facilitate supporting the specimen at the ends suitable supports were specially fabricated. These were fixed on a vibration table at a required spacing by T-bolts. The setup is shown in Figs. 2 and 3. Pressure of fluid is directly noted from the pressure gauge of the hand pump. Totally 36 specimens (including two virgin specimens, one each for the two materials) were considered for the vibration test. The same specimens were used for static deflection testing. Crack sizes in the range a/t = 0.22 to 0.57 for aluminium and 0.20 to 0.50 for mild steel, where a is edge crack size and t is pipe wall thickness, were examined. The cracks were generated through wire-cut machining. The wire diameter was 0.15 mm.

4.1 Deflection method

To facilitate determination of K through deflection measurements, deflections at the load point B and at free end C (Fig. 2) were measured for specimens with and without crack. For testing specimens with crack, fixing of the pipe was so done that the crack is always located at the fixed end D (Fig. 2). As expected the vertical or transverse deflections at locations B and C are the same. This procedure was repeated for all the specimens. For both aluminium and mild steel four crack sizes were examined and for each crack size, three crack positions were considered for displacement measurements. In each case a load of 98.1 N (≈10 kg) was applied in the transverse direction. For each crack size three span lengths L_{DB} are considered. For each L_{DB}, one stiffness is obtained. Since the rotational spring stiffness does not depend on span length L_{DB}, the average of these three values is taken as the representative rotational spring stiffness. These are shown in Table 1. The similar results, for mild steel, are shown in Table 2.

4.2 Vibration method

The problem of determination of the spring stiffness (K) can be handled in two ways. First, given a crack location β and natural frequency, K can be obtained straightway from Eq. (8) or (10). Second, the problem can be posed as a problem of determination of both K and crack location β from the knowledge of the frequencies. Since there are two unknowns (K and β) in this case, at least two relations are required between them for their determination. These are obtained through Eq. (8) or (10) using any two, may be the first two, natural frequencies. The intersection points of these two relations give all the possible combinations of K and β. A third relation between K and β, obtained through the third or any other unused natural frequency, is employed to decide on the unique pair. The intersection can be obtained graphically or through a numerical scheme like the bi-

Table 1 Measured rotational spring stiffness for aluminium pipes through deflection measurements

a/t	L_{c1}/L_{AB}	Empty pipe				Water filled pipe at pressure $p = 0$				Water filled pipe at pressure $p = 491$ kPa				Water filled pipe at pressure $p = 981$ kPa			
		δ_{nc}	δ_c	K	$K_{average}$	δ_{nc}	δ_c	K	$K_{average}$	δ_{nc}	δ_c	K	$K_{average}$	δ_{nc}	δ_c	K	$K_{average}$
		10^{-6}m	10^{-6}m	(kNm/rad)	(kNm/rad)	10^{-6}m	10^{-6}m	(kNm/rad)	(kNm/rad)	10^{-6}m	10^{-6}m	(kNm/rad)	(kNm/rad)	10^{-6}m	10^{-6}m	(kNm/rad)	(kNm/rad)
0.2286	0.245	7846	8674	25.650	24.478	7850	8745	24.081	23.975	7848	8626	27.091	26.032	7850	8649	25.788	27.351
	0.517	2030	2377	24.805		2031	2369	25.881		2033	2365	26.111		2032	2349	27.099	
	0.767	220	307	22.979		224	316	21.964		221	302	24.894		219	288	29.165	
0.3429	0.245	7846	9380	13.846	13.251	7850	9429	13.650	13.567	7848	9374	13.812	13.592	7850	9458	12.814	13.596
	0.517	2030	2694	13.010		2031	2659	13.930		2033	2670	13.609		2032	2650	13.901	
	0.767	220	375	12.898		224	378	13.121		221	372	13.354		219	362	14.073	
0.4571	0.245	7846	10073	9.538	9.219	7850	10154	9.355	9.367	7848	10042	9.606	9.451	7850	10087	9.211	9.365
	0.517	2030	2978	9.113		2031	2950	9.519		2033	2954	9.413		2032	2951	9.348	
	0.767	220	442	9.005		224	443	9.226		221	437	9.335		219	430	9.537	
0.5714	0.245	7846	10498	8.009	7.967	7850	10510	8.103	8.021	7848	10448	8.106	8.225	7850	10395	8.096	8.149
	0.517	2030	3124	7.896		2031	3124	8.004		2033	3077	8.304		2032	3079	8.205	
	0.767	220	470	7.997		224	478	7.955		221	465	8.264		219	466	8.147	

Table 2 Measured rotational spring stiffness for mild steel pipes through deflection measurements

a/t	L_{c1}/L_{AB}	Empty pipe				Water filled pipe at pressure $p = 0$				Water filled pipe at pressure $p = 491$ kPa				Water filled pipe at pressure $p = 981$ kPa			
		δ_{nc}	δ_c	K	$K_{average}$	δ_{nc}	δ_c	K	$K_{average}$	δ_{nc}	δ_c	K	$K_{average}$	δ_{nc}	δ_c	K	$K_{average}$
		10^{-6}m	10^{-6}m	(kNm/rad)	(kNm/rad)	10^{-6}m	10^{-6}m	(kNm/rad)	(kNm/rad)	10^{-6}m	10^{-6}m	(kNm/rad)	(kNm/rad)	10^{-6}m	10^{-6}m	(kNm/rad)	(kNm/rad)
0.20	0.513	804	1127	29.764	28.533	807	1188	25.451	26.207	809	1160	27.560	26.486	806	1174	26.222	25.053
	0.683	210	357	27.301		212	362	26.963		214	373	25.411		213	382	23.884	
0.30	0.513	804	1350	17.607	16.961	807	1428	15.615	16.062	809	1363	17.460	17.044	806	1394	16.411	15.362
	0.683	210	456	16.314		212	457	16.508		214	457	16.627		213	495	14.313	
0.40	0.343	1892	3505	11.005	11.604	1896	3454	11.501	11.764	1895	3372	12.081	11.989	1893	3512	11.033	10.692
	0.513	804	1598	12.108		807	1637	11.683		809	1608	12.107		806	1681	11.028	
	0.683	210	553	11.700		212	546	12.109		214	557	11.780		213	616	10.016	
0.50	0.343	1892	3864	9.002	9.001	1896	3760	9.613	9.728	1895	3855	9.104	9.199	1893	3941	8.722	8.480
	0.513	804	1860	9.104		807	1806	9.707		809	1848	9.310		806	1953	8.413	
	0.683	210	661	8.898		212	622	9.864		214	654	9.183		213	699	8.305	

section method. In the present study, the second strategy in conjunction with the graphical method has been employed. Therefore, while applying the method, the variation of K with β, corresponding to each of the three frequencies is obtained. The intersection of the three curves gives the required rotational spring stiffness and crack location. In case the three curves do not intersect exactly at a point, the center of gravity of the triangle formed by three-paired intersections is taken to obtain the most accurate K and β (Nandwana and Maiti 1997).

To measure the natural frequencies an accelerometer (Type 4374, Bruel & Kjaer, Denmark) with a mass of 0.65 gram, the lowest available in the laboratory, was glued on the specimen top during its testing using wax at a distance of 0.15 m from fixed end. The output of the accelerometer was amplified by a charge amplifier (Type 2635, Bruel & Kjaer, Denmark) and analyzed through a FFT analyzer (Type A&D-3524, Japan). The frequencies corresponding to the first few natural frequencies were obtained.

During the testing a pipe was lightly tapped by an impulse hammer in the transverse direction. The first few natural frequencies of specimens without and with crack were measured. The experimental data for the second, third and fourth frequencies are shown in Tables 3 to 6. The first

Table 3 Predicted stiffness and crack location for aluminum pipes through frequency measurements

Segment	Actual data		Natural frequencies (Hz)			Predicted data		
	β	a/t	ω_2	ω_3	ω_4	K (kNm/rad)	β	% error in β
			Empty pipe					
	No crack		65.16 68.67*	232.50 234.97*	614.69 624.78*			
1	0.245	0.2286	64.90	232.45	609.80	24.624	0.251	–0.60
		0.3429	64.70	232.40	606.00	13.733	0.252	–0.70
		0.4571	64.55	232.36	602.50	9.759	0.255	–1.00
		0.5714	64.35	232.25	599.00	7.392	0.254	–0.90
	0.517	0.2286	65.11	229.20	614.30	23.833	0.491	2.60
		0.3429	65.08	227.00	613.85	14.067	0.495	2.20
		0.4571	65.04	224.04	606.50	8.917	0.461	5.60
		0.5714	65.00	222.00	602.10	7.067	0.458	5.90
	0.767	0.2286	65.15	228.70	604.20	20.781	0.775	0.80
		0.3429	65.14	228.00	601.75	14.084	0.825	–5.80
		0.4571	65.13	227.05	598.60	8.963	0.846	–7.90
		0.5714	65.11	225.75	596.45	7.267	0.858	–9.10
2	0.412	0.2286	65.00	232.15	604.20	23.426	0.385	2.70
		0.3429	64.90	231.95	591.00	12.762	0.436	–2.40
		0.4571	64.81	231.60	583.66	8.565	0.425	1.30
		0.5714	64.75	231.50	580.63	7.892	0.415	0.30
	0.706	0.2286	65.13	232.40	608.75	24.019	0.642	6.40
		0.3429	65.12	232.35	605.80	13.561	0.665	4.10
		0.4571	65.11	232.28	602.45	9.856	0.674	3.20
		0.5714	65.09	232.22	598.20	8.428	0.658	4.80

Table 3 Continued

Segment	Actual data		Natural frequencies (Hz)			Predicted data		
	β	a/t	ω_2	ω_3	ω_4	K (kNm/rad)	β	% error in β
			Water filled pipe at no pressure $p = 0$					
	No crack		60.00 60.78*	206.25 207.97*	572.34 552.97*			
1	0.245	0.2286	59.75	206.20	568.00	27.028	0.255	–1.00
		0.3429	59.53	206.15	564.85	12.425	0.221	2.40
		0.4571	59.35	206.09	561.50	8.992	0.230	1.50
		0.5714	59.25	206.00	560.45	7.538	0.219	2.60
	0.517	0.2286	59.95	203.55	571.84	25.408	0.492	2.50
		0.3429	59.92	201.05	571.15	13.150	0.490	2.70
		0.4571	59.90	198.00	570.80	8.495	0.501	1.60
		0.5714	59.88	197.34	570.65	7.552	0.491	2.60
	0.767	0.2286	59.99	204.40	562.84	25.867	0.785	–1.80
		0.3429	59.98	202.84	554.60	12.025	0.825	–5.80
		0.4571	59.97	201.98	553.95	8.283	0.830	–6.30
		0.5714	59.96	200.75	552.35	7.481	0.815	–4.80
2	0.412	0.2286	59.87	205.97	562.20	24.820	0.421	–0.90
		0.3429	59.74	205.70	553.00	12.973	0.400	1.20
		0.4571	59.63	205.45	544.10	8.957	0.391	2.10
		0.5714	59.60	205.30	540.30	7.561	0.405	0.70
	0.706	0.2286	59.96	206.12	566.18	28.042	0.592	11.40
		0.3429	59.95	206.05	561.00	11.538	0.667	3.90
		0.4571	59.94	206.00	559.50	9.450	0.648	5.80
		0.5714	59.92	205.94	556.84	8.096	0.628	7.80

*-Natural frequency of pipe with no crack obtained by Eq. (7) or (9) using $K = \infty$.

frequency showed a minimal difference between the two cases, specimens with and without crack, and it has not been included. The first two tables present results for aluminium; the last two show the same for mild steel. The experimental and analytical frequencies for pipes with no crack are required for the zero setting, while solving an inverse problem (Nandwana and Maiti 1997). The frequencies of a pipe with no crack obtained by Eq. (7) or (9) using $K = \infty$ are shown in these tables.

The stiffnesses obtained through the inverse analysis are shown in Tables 3 and 4 for aluminium and Tables 5 and 6 for mild steel pipes. Typical variation of K with β, where β = AD/AB for a crack in segment AB (Fig. 1), is shown in Fig. 4.

5. Results and discussion

Based on the results (Tables 1 and 2) of the deflection method, it is found that the stiffness of

Table 4 Predicted stiffness and crack location for aluminum pipes through frequency measurements

Segment	Actual data		Natural frequencies (Hz)			Predicted data		
	β	a/t	ω_2	ω_3	ω_4	K (kNm/rad)	β	% error in β
			Water filled pipe at pressure p = 491 kPa					
	No crack		61.25	207.19	572.72			
			60.79*	208.19*	553.24*			
1	0.245	0.2286	61.00	207.18	568.50	25.681	0.239	0.60
		0.3429	60.82	207.16	564.85	14.068	0.244	0.10
		0.4571	60.65	207.13	561.40	8.992	0.231	1.40
		0.5714	60.58	207.10	560.35	8.106	0.252	–0.70
	0.517	0.2286	61.23	203.10	570.88	25.136	0.488	2.90
		0.3429	61.21	200.00	569.63	13.562	0.485	3.20
		0.4571	61.18	198.56	568.80	9.117	0.480	3.70
		0.5714	61.15	197.00	567.45	7.183	0.498	1.90
	0.767	0.2286	61.24	204.78	563.45	21.082	0.845	–7.80
		0.3429	61.23	202.67	556.00	11.254	0.836	–6.90
		0.4571	61.22	201.00	549.40	8.769	0.825	–5.80
		0.5714	61.21	200.55	549.00	7.257	0.830	–6.30
2	0.412	0.2286	61.12	206.90	562.60	24.062	0.406	0.60
		0.3429	61.00	206.65	553.30	12.977	0.409	0.30
		0.4571	60.85	206.45	544.00	9.387	0.398	1.40
		0.5714	60.70	206.33	540.20	8.120	0.365	4.70
	0.706	0.2286	61.21	207.05	565.31	25.421	0.586	12.0
		0.3429	61.19	206.93	560.00	13.658	0.615	9.10
		0.4571	61.16	206.85	555.10	10.028	0.581	12.50
		0.5714	61.10	206.60	545.15	8.062	0.575	13.10
			Water filled pipe at pressure p = 981 kPa					
	No crack		62.03	208.91	575.31			
			60.81*	208.42*	553.52*			
1	0.245	0.2286	61.79	208.89	571.00	28.420	0.240	0.50
		0.3429	61.60	208.85	567.30	13.856	0.248	–0.30
		0.4571	61.40	208.82	564.25	8.921	0.248	–0.30
		0.5714	61.34	208.77	563.05	8.254	0.247	–0.20
	0.517	0.2286	62.01	205.30	574.80	24.510	0.508	0.90
		0.3429	62.00	200.65	574.23	12.258	0.522	–0.50
		0.4571	61.98	197.20	573.75	8.852	0.510	0.70
		0.5714	61.96	196.85	573.45	7.451	0.501	1.60
	0.767	0.2286	62.02	206.50	566.00	21.085	0.825	–5.80
		0.3429	62.00	204.42	559.65	11.684	0.842	–7.50
		0.4571	61.98	203.60	555.75	8.725	0.836	–6.90
		0.5714	61.97	202.85	553.20	7.315	0.856	–8.90
2	0.412	0.2286	61.90	208.60	565.15	24.583	0.409	0.30
		0.3429	61.75	208.40	556.10	13.821	0.387	2.50
		0.4571	61.66	208.12	546.00	8.927	0.390	2.20
		0.5714	61.60	208.00	544.10	8.037	0.398	1.40
	0.706	0.2286	61.99	208.77	567.92	23.892	0.598	10.80
		0.3429	61.94	208.65	560.10	14.462	0.575	13.10
		0.4571	61.90	208.50	553.75	10.412	0.568	13.80
		0.5714	61.88	208.40	548.60	7.682	0.572	13.4

*-Natural frequency of pipe with no crack obtained by Eq. (7) or (9) using $K = \infty$.

Table 5 Predicted stiffness and crack location for mild steel pipes through frequency measurements

Segment	Actual data		Natural frequencies (Hz)			Predicted data		
	β	a/t	ω_2	ω_3	ω_4	K (kNm/rad)	β	% error in β
			Empty pipe					
	No crack		62.50	211.56	586.56			
			64.77*	223.18*	592.93*			
1	0.343	0.40	61.55	207.40	546.00	10.565	0.311	3.20
		0.50	61.40	204.45	540.68	8.534	0.324	1.90
	0.513	0.20	62.45	200.00	584.10	24.996	0.507	0.60
		0.30	62.41	197.20	583.50	16.417	0.501	1.20
		0.40	62.35	195.85	582.95	12.721	0.495	1.80
		0.50	62.28	192.10	579.80	9.483	0.485	2.80
	0.683	0.20	62.48	202.50	576.15	23.426	0.624	5.90
		0.30	62.47	199.00	573.46	16.333	0.601	8.20
		0.40	62.46	192.02	569.05	10.264	0.596	8.70
		0.50	62.44	190.78	567.46	9.288	0.598	8.50
2	0.485	0.20	62.28	210.87	559.00	24.109	0.496	–1.10
		0.30	62.11	210.48	541.56	16.483	0.462	2.30
		0.40	61.95	210.06	517.91	11.425	0.472	1.30
		0.50	61.80	209.45	505.37	8.740	0.464	2.10
			Water filled pipe at no pressure $p = 0$					
	No crack		58.75	200.31	564.38			
			62.79*	216.35*	574.78*			
1	0.343	0.40	58.10	193.35	524.00	10.621	0.340	0.30
		0.50	57.94	191.75	517.60	8.608	0.339	0.40
	0.513	0.20	58.70	190.26	563.75	24.153	0.524	–1.10
		0.30	58.66	185.71	561.28	15.430	0.508	0.50
		0.40	58.64	178.60	559.87	10.724	0.502	1.10
		0.50	58.60	175.57	557.82	8.847	0.501	1.20
	0.683	0.20	58.73	193.00	558.87	29.667	0.590	9.30
		0.30	58.72	188.12	547.63	17.167	0.601	8.20
		0.40	58.71	184.36	538.28	11.267	0.621	6.20
		0.50	58.69	179.77	534.59	8.592	0.596	8.70
2	0.485	0.20	58.52	199.67	537.68	25.752	0.467	1.80
		0.30	58.40	199.35	520.00	16.575	0.452	3.30
		0.40	58.21	198.90	497.20	11.426	0.471	1.40
		0.50	58.08	198.40	479.55	8.560	0.463	2.20

*-Natural frequency of pipe with no crack obtained by Eq. (7) or (9) using $K = \infty$.

pipe filled with water under pressure (0, 491 kPa and 981 kPa), differ from that of the empty pipe at the most by –2.38%, –6.35%, –11.74% for aluminium and 8.15%, 7.17%, 12.2% for mild steel respectively. For the two water pressures (491 kPa and 981 kPa), the stiffnesses differ from that of

Table 6 Predicted stiffness and crack location for mild steel pipes through frequency measurements

Segment	Actual data		Natural frequencies (Hz)			Predicted data		
	β	a/t	ω_2	ω_3	ω_4	K (kNm/rad)	β	% error in β
			Water filled pipe at pressure p = 491 kPa					
	No crack		58.91	200.94	564.69			
			62.79*	216.41*	574.85*			
1	0.343	0.40	58.25	193.70	525.00	10.621	0.335	0.80
		0.50	58.16	191.65	518.19	8.706	0.332	1.10
	0.513	0.20	58.86	190.10	562.60	24.862	0.524	–1.10
		0.30	58.82	185.75	562.18	14.333	0.507	0.60
		0.40	58.79	181.56	561.65	10.851	0.519	–0.60
		0.50	58.76	178.06	560.53	8.607	0.508	0.50
	0.683	0.20	58.89	193.63	558.30	28.250	0.592	9.10
		0.30	58.87	188.42	547.00	15.028	0.614	6.90
		0.40	58.85	185.23	542.82	10.983	0.595	8.80
		0.50	58.82	182.10	539.64	8.933	0.599	8.40
2	0.485	0.20	58.68	200.26	538.00	24.867	0.465	2.00
		0.30	58.55	199.85	524.63	16.205	0.448	3.70
		0.40	58.36	199.45	502.05	11.658	0.452	3.30
		0.50	58.23	199.00	482.16	8.767	0.460	2.50
			Water filled pipe at pressure p = 981 kPa					
	No crack		59.38	202.19	565.94			
			62.80*	216.47*	574.93*			
1	0.343	0.40	58.70	196.42	526.23	11.068	0.332	1.10
		0.50	58.55	194.62	520.45	9.056	0.330	1.30
	0.513	0.20	59.32	193.28	564.30	25.333	0.507	0.60
		0.30	59.29	187.80	563.65	15.067	0.505	0.80
		0.40	59.25	182.00	562.40	10.892	0.500	1.30
		0.50	59.22	180.65	561.86	9.103	0.509	0.40
	0.683	0.20	59.36	195.45	557.87	29.028	0.597	8.60
		0.30	59.37	188.34	545.60	15.316	0.604	7.90
		0.40	59.35	185.00	540.50	10.562	0.625	5.80
		0.50	59.33	181.21	538.00	8.620	0.614	6.90
2	0.485	0.20	59.15	201.55	539.40	26.067	0.459	2.60
		0.30	59.02	201.25	520.20	16.626	0.472	1.30
		0.40	58.83	200.68	504.13	11.901	0.455	3.00
		0.50	58.73	200.30	484.00	8.830	0.473	1.30

*-Natural frequency of pipe with no crack obtained by Eq. (7) or (9) using $K = \infty$.

the water filled pipe at no pressure by at the most –8.58% and –14.08% respectively for aluminium, –6.11% and 12.83% respectively for mild steel.

Based on the observations (Tables 3 to 6) of the vibration method, stiffness in the case of pipe

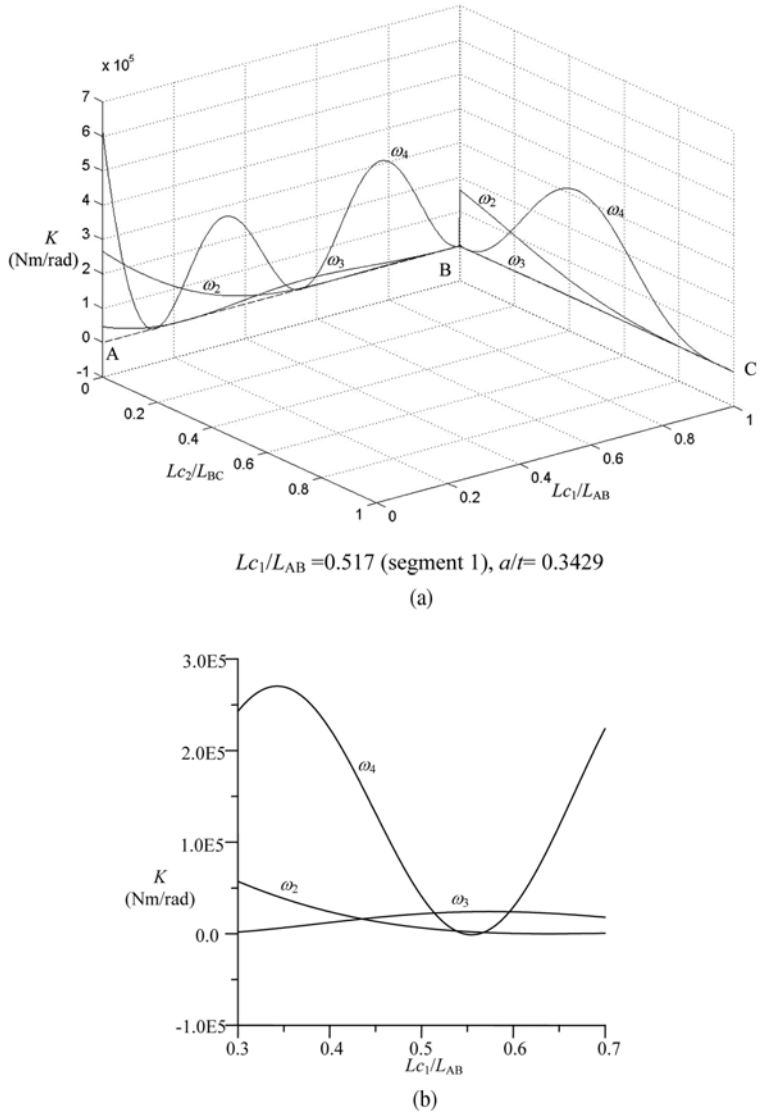

Fig. 4 Plot of stiffness K vs. crack location β for aluminium empty pipe. (a) 3-D view, (b) Enlarged portion at crack location

filled with water under pressure (0, 491 kPa and 981 kPa), differ with that of the empty pipe at the most by 6.63%, –6.92% –2.32% for aluminium and 4.75%, –13.02%, 6.71% for mild steel respectively. For the two water pressures (491 kPa and 981 kPa), the stiffnesses differ from that of the water filled pipe at no pressure by at the most –3.13% and –5.37% respectively for aluminium and –16.96% and –7.92% respectively for steel. The stiffness obtained by the frequency method differs from that obtained through deflection techniques by –6.29% and –5.98% for empty and water filled aluminium pipes respectively. The similar differences for the mild steel pipes are 12.40% and 9.06% respectively.

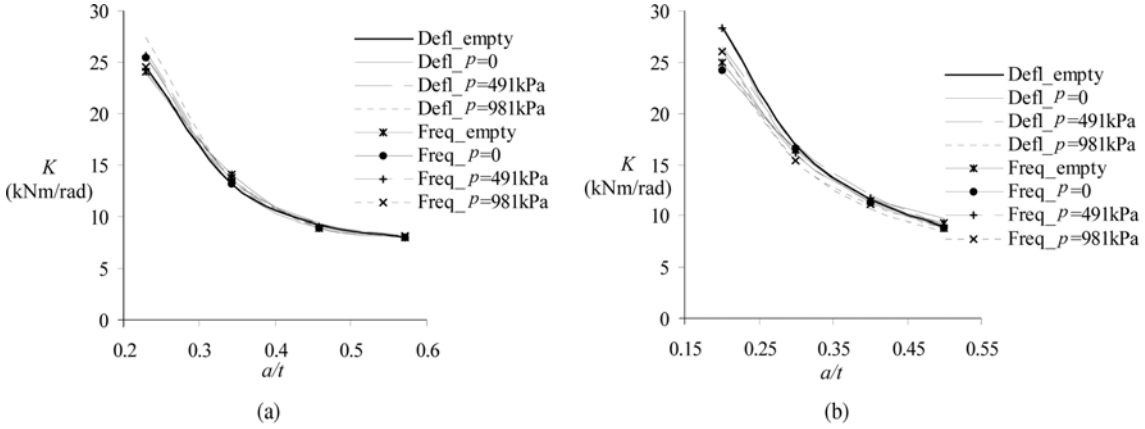

Fig. 5 Comparison of variation of stiffness K vs. crack size a/t for (a) aluminium and (b) mild steel pipes obtained by two methods for different internal conditions

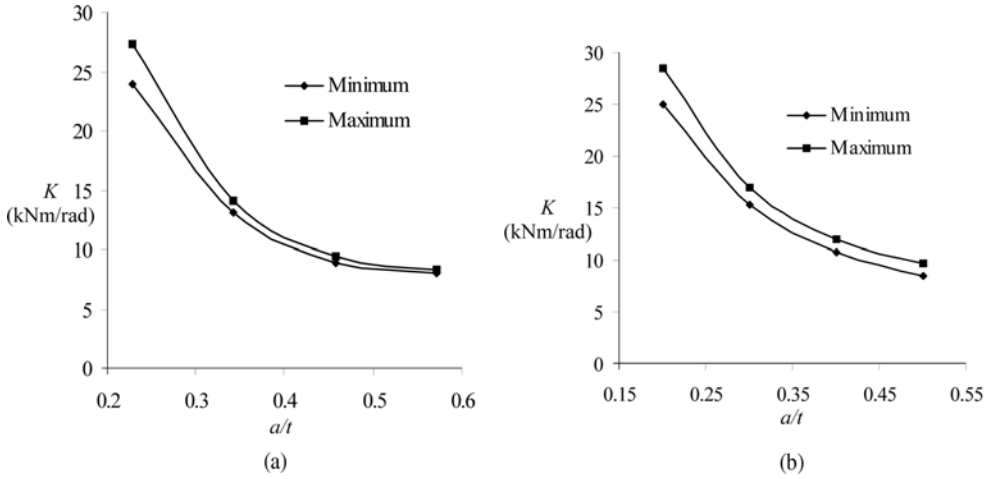

Fig. 6 Variation band of stiffness K vs. crack size a/t for (a) aluminium and (b) mild steel pipes

The results by the two methods are therefore very close. The variations of rotational spring stiffness with crack size are shown in Fig. 5. These results are combined to show the band in variation in Fig. 6. Since, a closed form relation between the rotational spring stiffness and crack size is not available, these plots can be very helpful in crack detection; crack size can be obtained given a spring stiffness.

Variations of rotational spring stiffness K with crack location β (Fig. 4) helps to predict the crack location as well. The results so obtained are presented in Tables 3 to 6. The maximum errors are 13.80% and 9.30% for aluminium and mild steel pipes respectively. The vibration method can therefore be employed for the prediction of crack location.

The crack size has been predicted using Fig. 6. These are shown in Tables 7 to 10. The error in size lies in the range –17.24% to 14.95% for aluminium and –16.90% to 13.00% for mild steel.

The accuracy of prediction of crack location and crack size are both dependent on the accuracy of

Table 7 Accuracy of prediction of crack size in aluminium pipes

Segment	Actual		Predicted crack data				
	β	a/t	K (kNm/rad)	a/t		% error in a/t	
				Min.	Max.	Min.	Max.
			Empty pipe				
1	0.245	0.2286	24.624	0.2250	0.2422	1.57	–5.95
		0.3429	13.733	0.3335	0.3485	2.74	–1.63
		0.4571	9.759	0.4240	0.4448	7.24	2.69
		0.5714	7.392	0.6160	0.6386	–7.81	–11.76
	0.517	0.2286	23.833	0.2292	0.2458	–0.26	–7.52
		0.3429	14.067	0.3280	0.3430	4.35	–0.03
		0.4571	8.917	0.4576	0.4855	–0.11	–6.21
		0.5714	7.067	0.6457	0.6681	–13.00	–16.92
	0.767	0.2286	20.781	0.2512	0.2680	–9.89	–17.24
		0.3429	14.084	0.3278	0.3427	4.40	0.06
		0.4571	8.963	0.4570	0.4848	0.02	–6.06
		0.5714	7.267	0.6269	0.6497	–9.71	–13.70
2	0.412	0.2286	23.426	0.2315	0.2481	–1.27	–8.53
		0.3429	12.762	0.3500	0.3672	–2.07	–7.09
		0.4571	8.565	0.4763	0.5138	–4.20	–12.40
		0.5714	7.892	0.5775	0.5965	–1.07	–4.39
	0.706	0.2286	24.019	0.2285	0.2440	0.04	–6.74
		0.3429	13.561	0.3361	0.3518	1.98	–2.60
		0.4571	9.856	0.4211	0.4411	7.88	3.50
		0.5714	8.428	0.4860	0.5300	14.95	7.25
			Water filled pipe at no pressure $p = 0$				
1	0.245	0.2286	27.028	0.2160	0.2293	5.51	–0.31
		0.3429	12.425	0.3571	0.3733	–4.14	–8.87
		0.4571	8.992	0.4539	0.4820	0.70	–5.45
		0.5714	7.538	0.6042	0.6264	–5.74	–9.63
	0.517	0.2286	25.408	0.2225	0.2365	2.67	–3.46
		0.3429	13.150	0.3433	0.3592	–0.12	–4.75
		0.4571	8.495	0.4825	0.5216	–5.56	–14.11
		0.5714	7.552	0.6031	0.6235	–5.55	–9.12
	0.767	0.2286	25.867	0.2201	0.2343	3.72	–2.49
		0.3429	12.025	0.3646	0.3823	–6.33	–11.49
		0.4571	8.283	0.4998	0.5227	–9.34	–14.35
		0.5714	7.481	0.6108	0.6308	–6.90	–10.40
2	0.412	0.2286	24.820	0.2245	0.2393	1.79	–4.68
		0.3429	12.973	0.3465	0.3625	–1.05	–5.72
		0.4571	8.957	0.4573	0.4849	–0.04	–6.08
		0.5714	7.561	0.6026	0.6244	–5.46	–9.28
	0.706	0.2286	28.042	0.2156	0.2263	5.69	1.01
		0.3429	11.538	0.3755	0.3934	–9.51	–14.73
		0.4571	9.450	0.4350	0.4575	4.83	–0.09
		0.5714	8.096	0.5226	0.5830	8.54	–2.03

Table 8 Accuracy of prediction of crack size in aluminium pipes

Segment	Actual		Predicted crack data				
	β	a/t	K (kNm/rad)	a/t Min.	a/t Max.	% error in a/t Min.	% error in a/t Max.
			Water filled pipe at pressure p = 491 kPa				
1	0.245	0.2286	25.681	0.2249	0.2390	1.62	–4.55
		0.3429	14.068	0.3276	0.3426	4.46	0.09
		0.4571	8.992	0.4539	0.4820	0.70	–5.45
		0.5714	8.106	0.5188	0.5821	9.21	–1.87
	0.517	0.2286	25.136	0.2201	0.2339	3.72	–2.32
		0.3429	13.562	0.3360	0.3518	2.01	–2.60
		0.4571	9.117	0.4485	0.4736	1.88	–3.61
		0.5714	7.183	0.6345	0.6580	–11.04	–15.16
	0.767	0.2286	21.082	0.2477	0.2642	–8.36	–15.57
		0.3429	11.254	0.3822	0.3998	–11.46	–16.59
		0.4571	8.769	0.4650	0.4956	–1.73	–8.42
		0.5714	7.257	0.6277	0.6505	–9.85	–13.84
2	0.412	0.2286	24.062	0.2280	0.2436	0.26	–6.56
		0.3429	12.977	0.3463	0.3625	–0.99	–5.72
		0.4571	9.387	0.4373	0.4602	4.33	–0.68
		0.5714	8.120	0.5182	0.5819	9.31	–1.84
	0.706	0.2286	25.421	0.2223	0.2361	2.76	–3.28
		0.3429	13.658	0.3340	0.3498	2.60	–2.01
		0.4571	10.028	0.4154	0.4350	9.12	4.83
		0.5714	8.062	0.5335	0.5834	6.63	–2.10
			Water filled pipe at pressure p = 981 kPa				
1	0.245	0.2286	28.420	0.2151	0.2262	5.91	1.05
		0.3429	13.856	0.3319	0.3469	3.21	–1.17
		0.4571	8.921	0.4575	0.4853	–0.09	–6.17
		0.5714	8.254	0.5030	0.5715	11.97	–0.02
	0.517	0.2286	24.510	0.2252	0.2425	1.49	–6.08
		0.3429	12.258	0.3600	0.3771	–4.99	–9.97
		0.4571	8.852	0.4613	0.4899	–0.92	–7.18
		0.5714	7.451	0.6112	0.6332	–6.97	–10.82
	0.767	0.2286	21.085	0.2488	0.2656	–8.84	–16.19
		0.3429	11.684	0.3725	0.3899	–8.63	–13.71
		0.4571	8.725	0.4685	0.5000	–2.49	–9.39
		0.5714	7.315	0.6225	0.6450	–8.94	–12.88
2	0.412	0.2286	24.583	0.2250	0.2404	1.57	–5.16
		0.3429	13.821	0.3322	0.3470	3.12	–1.20
		0.4571	8.927	0.4574	0.4852	–0.07	–6.15
		0.5714	8.037	0.5325	0.5928	6.81	–3.75
	0.706	0.2286	23.892	0.2291	0.2450	–0.22	–7.17
		0.3429	14.462	0.3223	0.3373	6.01	1.63
		0.4571	10.412	0.4045	0.4245	11.51	7.13
		0.5714	7.682	0.5941	0.6145	–3.97	–7.54

Table 9 Accuracy of prediction of crack size in mild steel pipes

Segment	Actual		Predicted crack data				
	β	a/t	K (kNm/rad)	a/t Min.	a/t Max.	% error in a/t Min.	% error in a/t Max.
			Empty pipe				
1	0.343	0.40	10.565	0.4041	0.4523	–1.02	–13.07
		0.50	8.534	0.4974	0.5705	0.52	–14.10
	0.513	0.20	24.996	0.2004	0.2221	–0.20	–11.05
		0.30	16.417	0.2839	0.3090	5.37	–3.00
		0.40	12.721	0.3480	0.3802	13.00	4.95
		0.50	9.483	0.4458	0.5195	10.84	–3.90
	0.683	0.20	23.426	0.2115	0.2338	–5.75	–16.90
		0.30	16.333	0.2856	0.3106	4.80	–3.53
		0.40	10.264	0.4145	0.4672	–3.62	–16.80
		0.50	9.288	0.4548	0.5275	9.04	–5.50
2	0.485	0.20	24.109	0.2063	0.2285	–3.15	–14.25
		0.30	16.483	0.2835	0.3085	5.50	–2.83
		0.40	11.425	0.3790	0.4175	5.25	–4.37
		0.50	8.740	0.4831	0.5573	3.38	–11.46
			Water filled at no pressure $p = 0$				
1	0.343	0.40	10.621	0.4015	0.4490	–0.38	–12.25
		0.50	8.608	0.4905	0.5662	1.90	–13.24
	0.513	0.20	24.153	0.2060	0.2281	–3.00	–14.05
		0.30	15.430	0.2985	0.3250	0.50	–8.33
		0.40	10.724	0.3985	0.4446	0.38	–11.15
		0.50	8.847	0.4765	0.5508	4.70	–10.16
	0.683	0.20	29.667	0.1775	0.1955	11.25	2.25
		0.30	17.167	0.2744	0.2986	8.53	0.47
		0.40	11.267	0.3838	0.4238	4.05	–5.95
		0.50	8.592	0.4923	0.5673	1.54	–13.46
2	0.485	0.20	25.752	0.1960	0.2163	2.00	–8.15
		0.30	16.575	0.2825	0.3074	5.83	–2.47
		0.40	11.426	0.4080	0.4175	–2.00	–4.37
		0.50	8.560	0.4949	0.5690	1.02	–13.80

measurement of the natural frequencies. The accuracy of prediction of the crack location is reasonably good, but the accuracy of the prediction of crack size is not that good. One reason for this is that graphical relation between the rotational spring stiffness K and crack size a obtained through experiment has been utilized to predict a from K. With the availability of a close form relation between the two the accuracy will improve.

6. Conclusions

The modelling scheme proposed by Murigendrappa (2004) for analysis of free out-of-plane

Table 10 Accuracy of prediction of crack size in mild steel pipes

Segment	Actual		Predicted crack data				
	β	a/t	K (kNm/rad)	a/t Min.	a/t Max.	% error in a/t Min.	% error in a/t Max.
Water filled at pressure p = 491 kPa							
1	0.343	0.40	10.621	0.4020	0.4471	–0.50	–11.77
		0.50	8.706	0.4846	0.5592	3.08	–11.84
	0.513	0.20	24.862	0.2012	0.2230	–0.60	–11.50
		0.30	14.333	0.3166	0.3450	–5.53	–15.00
		0.40	10.851	0.3960	0.4395	1.00	–9.87
		0.50	8.607	0.4908	0.5661	1.84	–13.22
	0.683	0.20	28.250	0.1838	0.2016	8.10	–0.80
		0.30	15.028	0.3043	0.3321	–1.43	–10.70
		0.40	10.983	0.3921	0.4347	1.98	–8.67
		0.50	8.933	0.4708	0.5458	5.84	–9.16
2	0.485	0.20	24.867	0.2010	0.2228	–0.50	–11.40
		0.30	16.205	0.2874	0.3125	4.20	–4.17
		0.40	11.658	0.3738	0.4105	6.55	–2.62
		0.50	8.767	0.4819	0.5530	3.62	–10.60
Water filled at pressure p = 981 kPa							
1	0.343	0.40	11.068	0.3894	0.4313	2.65	–7.82
		0.50	9.056	0.4654	0.5390	6.92	–7.80
	0.513	0.20	25.333	0.1988	0.2190	0.60	–9.50
		0.30	15.067	0.3041	0.3320	–1.37	–10.67
		0.40	10.892	0.3945	0.4343	1.38	–8.57
		0.50	9.103	0.4625	0.5354	7.50	–7.08
	0.683	0.20	29.028	0.1789	0.1985	10.55	0.75
		0.30	15.316	0.2996	0.3271	0.13	–9.03
		0.40	10.562	0.4040	0.4525	–1.00	–13.12
		0.50	8.620	0.4900	0.5659	2.00	–13.18
2	0.485	0.20	26.067	0.1963	0.2140	1.85	–7.00
		0.30	16.626	0.2815	0.3063	6.17	–2.10
		0.40	11.901	0.3675	0.4030	8.13	–0.75
		0.50	8.830	0.4783	0.5514	4.34	–10.28

transverse vibration of crack-free L-shaped pipes filled with fluid under pressure by invoking suitable torsional springs at the knee permits study of similar pipes with crack. Such modelling enables detection of crack provided the relationship between crack size and crack-equivalent rotational spring is known. The crack size equivalent rotational spring stiffness is determined experimentally by two methods, one based on displacement measurements and the other based on the frequency measurement and inverse vibration analysis. The results by the two methods differ in magnitude at the most by 6.29% and 12.4% for aluminium and steel pipes. The variation of rotational spring stiffness with crack size is obtained for the range $a = 0.22t$ to $0.57t$ for aluminium

and $0.2t$ to $0.5t$ for steel. These plots can be utilized for the prediction of crack sizes. Crack located in both the segments is considered for the prediction. The maximum absolute error in the prediction of location is 13.80%. The maximum absolute error in the prediction of crack size is 17.24% for aluminium and 16.90% for mild steel. One of the reasons for this higher error in the case of crack size is the employment of graphical relation between the spring stiffness and crack size obtained experimentally.

References

Bovsunovsky, A.P. and Matveev, V.V. (2000), "Analytical approach to the determination of dynamic characteristics of a beam with a closing crack", *J. Sound Vib.*, **235**(3), 415-435.

Chaudhari, T.D. and Maiti, S.K. (2000), "Experimental verification of a method of detection of crack in taper and segmented beams based on modeling of transverse vibration", *Int. J. of Fracture,* **102**, L33-L38.

Chaudhari, T.D. (2000), "Modelling of transverse vibration of geometrically segmented beams to facilitate crack detection", Ph.D. Thesis, Department of Mechanical Engineering, Indian Institute of Technology Bombay.

Chondros, T.G. and Dimarogonas, A.D. (1989), "Dynamic sensitivity of structures to cracks", Transactions of the ASME Journal of Vibration, Acoustics, Stress and Reliability in Design, **111**, 251-256.

Choy, F.K., Liang, R. and Xu, P. (1995), "Fault identification in beams on elastic foundation", *Computers Geotechnics* **17**(2), 157-176.

Dimarogonas, A.D. (1996), "Vibration of cracked structures: A state of the art review", *Engineering Fracture Mechanics*, **55**(5), 831-857.

Doebling, S.W., Farrar, C.E. and Prime, M.B. (1998), "A summary review of vibration-based damage identification methods", *The Shock and Vibration Digest*, **30**(2), 91-105.

Gasch, R. (1993), "A survey of the dynamic behavior of a simple rotating shaft with a transverse crack", *J. Sound Vib.*, **160**(2), 313-332.

Hassiotis, S. and Jeong, G.D. (1993), "Assessment of structural damage from natural frequency measurement", *Comput. Struct.*, **49**(4), 679-691.

Hassiotis, S. (1999), "Identification of damage using natural frequencies and system moments", *Struct. Eng. Mech.*, **8**(3), 285-297.

Hu, J. and Liang, R.Y. (1993), "An Integrated approach to detection of cracks using vibration characteristics", *J. of the Franklin Institute*, **330**(5), 841-853.

Kim, J.-T. and Stubbs, N. (2003), "Crack detection in beam-type structures using frequency data", *J. Sound Vib.*, **259**(1), 145-160.

Li, Q.S. (2002), "Free vibration analysis of non-uniform beams with an arbitrary number of cracks and concentrated masses", *J. Sound Vib.*, **252**(3), 509-525.

Liang, R.Y., Choy, F.K. and Hu, J. (1991), "Detection of cracks in beam structures using measurements of natural frequencies", *J. of the Franklin Institute*, **328**, 505-518.

Morassi, A. and Rovere, N. (1997), "Localizing a notch in a steel frame from frequency measurements", *J. Eng. Mech.*, **123**, 422-432.

Murigendrappa, S.M., Maiti, S.K. and Srirangarajan, H.R. (2004), "Experimental and theoretical study on crack detection in pipes filled with fluid", *J. Sound Vib.*, **270**(4-5), 1013-1032.

Murigendrappa, S.M. (2004), "Detection of crack in straight and L-shaped pipes filled with fluid based on transverse natural frequencies", Ph.D. Thesis, Department of Mechanical Engineering, Indian Institute of Technology Bombay.

Nandwana, B.P. and Maiti, S.K. (1997), "Modelling of vibration of beam in presence of inclined edge and internal crack for its possible detection based on frequency measurements", *Engineering Fracture Mechanics*, **58**(3), 193-205.

Narkis, Y. (1994), "Identification of crack location in vibrating simply supported beam", *J. Sound Vib.*, **172**(4), 549-558.

Nikolakopoulos, P.G., Katsareas, D.E. and Papadopoulos, C.A. (1997), "Crack identification in frame structures",

Comput. Struct., **64**(1-4), 389-406.
Patil, D.P. and Maiti, S.K. (2002), "An approach for crack detection in beams on elastic foundations using frequency measurements", *Int. J. of Acoustics and Vibration,* **7**, 243-249.
Ruotolo, R. and Surace, C. (1997), "Damage assessment of multiple cracked beams: Numerical results and experimental validation", *J. Sound Vib.*, **206**(4), 567-588.
Saavedra, P.N. and Cuitiño, L.A. (2001), "Crack detection and vibration behaviour of cracked beams", *Comput. Struct.*, **79**, 1451-1459.
Salawu, O.S. (1997), "Detection of structural damage through changes in frequency: A review", *Eng. Struct.*, **19**(9), 718-723.
Shi, Z.Y., Law, S.S. and Zhang, L.M. (1998), "Structural damage localization from modal strain energy change", *J. Sound Vib.*, **218**(5), 825-844.
Wauer, J. (1990), "On the dynamics of cracked rotors: A literature survey", *Applied Mechanics Review*, **43**(1), 13-17.
Xia, Y. and Hao, H. (2000), "Measurement selection for vibration-based structural damage identification", *J. Sound Vib.*, **236**(1), 89-104.
Yao G.C., Chang K.C. and Lee, G.C. (1992), "Damage diagnosis of steel frames using vibration signature analysis", *J. Eng. Mech.*, **118**(9), 1949-1961.

Appendix I: A_{ij} and B_{ij} involved in Eqs. (7) and (8).

$$A_{11} = T_{31}^{(3)}[T_{13}^{(1)}T_{11}^{(2)} + T_{23}^{(1)}T_{12}^{(2)} + T_{33}^{(1)}T_{13}^{(2)} + T_{43}^{(1)}T_{14}^{(2)}] + T_{34}^{(3)}[T_{13}^{(1)}T_{41}^{(2)} + T_{23}^{(1)}T_{42}^{(2)} + T_{33}^{(1)}T_{43}^{(2)} + T_{43}^{(1)}T_{44}^{(2)}]$$

$$A_{12} = T_{31}^{(3)}[T_{14}^{(1)}T_{11}^{(2)} + T_{24}^{(1)}T_{12}^{(2)} + T_{34}^{(1)}T_{13}^{(2)} + T_{44}^{(1)}T_{14}^{(2)}] + T_{34}^{(3)}[T_{14}^{(1)}T_{41}^{(2)} + T_{24}^{(1)}T_{42}^{(2)} + T_{34}^{(1)}T_{43}^{(2)} + T_{44}^{(1)}T_{44}^{(2)}]$$

$$A_{13} = T_{32}^{(3)}\left\{\left(\frac{L_1}{GJ} - \frac{L_2}{GJ}\right) - \frac{L_{AB}}{GJ}\right\} - T_{33}^{(3)}$$

$$A_{21} = T_{41}^{(3)}[T_{13}^{(1)}T_{11}^{(2)} + T_{23}^{(1)}T_{12}^{(2)} + T_{33}^{(1)}T_{13}^{(2)} + T_{43}^{(1)}T_{14}^{(2)}] + T_{44}^{(3)}[T_{13}^{(1)}T_{41}^{(2)} + T_{23}^{(1)}T_{42}^{(2)} + T_{33}^{(1)}T_{43}^{(2)} + T_{43}^{(1)}T_{44}^{(2)}]$$

$$A_{22} = T_{41}^{(3)}[T_{14}^{(1)}T_{11}^{(2)} + T_{24}^{(1)}T_{12}^{(2)} + T_{34}^{(1)}T_{13}^{(2)} + T_{44}^{(1)}T_{14}^{(2)}] + T_{44}^{(3)}[T_{14}^{(1)}T_{41}^{(2)} + T_{24}^{(1)}T_{42}^{(2)} + T_{34}^{(1)}T_{43}^{(2)} + T_{44}^{(1)}T_{44}^{(2)}]$$

$$A_{23} = T_{42}^{(3)}\left\{\left(\frac{L_1}{GJ} - \frac{L_2}{GJ}\right) - \frac{L_{AB}}{GJ}\right\} - T_{43}^{(3)}$$

$$A_{31} = -[T_{13}^{(1)}T_{31}^{(2)} + T_{23}^{(1)}T_{32}^{(2)} + T_{33}^{(1)}T_{33}^{(2)} + T_{43}^{(1)}T_{34}^{(2)}],\ A_{32} = -[T_{14}^{(1)}T_{31}^{(2)} + T_{24}^{(1)}T_{32}^{(2)} + T_{34}^{(1)}T_{33}^{(2)} + T_{44}^{(1)}T_{34}^{(2)}]$$

$$B_{11} = T_{33}^{(1)}T_{12}^{(2)}T_{31}^{(3)} + T_{33}^{(1)}T_{42}^{(2)}T_{34}^{(3)},\ B_{12} = T_{34}^{(1)}T_{12}^{(2)}T_{31}^{(3)} + T_{34}^{(1)}T_{42}^{(2)}T_{34}^{(3)},\ B_{21} = T_{33}^{(1)}T_{12}^{(2)}T_{41}^{(3)} + T_{33}^{(1)}T_{42}^{(2)}T_{44}^{(3)}$$

$$B_{22} = T_{34}^{(1)}T_{12}^{(2)}T_{41}^{(3)} + T_{34}^{(1)}T_{42}^{(2)}T_{44}^{(3)},\ B_{31} = T_{33}^{(1)}T_{32}^{(2)},\ B_{32} = T_{34}^{(1)}T_{32}^{(2)}$$

Appendix II: A_{ij} and B_{ij} involved in Eqs. (9) and (10).

$$A_{11} = T_{31}^{(3)}[T_{13}^{(1)}T_{11}^{(2)} + T_{43}^{(1)}T_{14}^{(2)}] + T_{32}^{(3)}[T_{13}^{(1)}T_{21}^{(2)} + T_{43}^{(1)}T_{24}^{(2)}] + T_{33}^{(3)}[T_{13}^{(1)}T_{31}^{(2)} + T_{43}^{(1)}T_{34}^{(2)}] + T_{34}^{(3)}[T_{13}^{(1)}T_{41}^{(2)} + T_{43}^{(1)}T_{44}^{(2)}]$$

$$A_{12} = T_{31}^{(3)}[T_{14}^{(1)}T_{11}^{(2)} + T_{44}^{(1)}T_{14}^{(2)}] + T_{32}^{(3)}[T_{14}^{(1)}T_{21}^{(2)} + T_{44}^{(1)}T_{24}^{(2)}] + T_{33}^{(3)}[T_{14}^{(1)}T_{31}^{(2)} + T_{44}^{(1)}T_{34}^{(2)}] + T_{34}^{(3)}[T_{14}^{(1)}T_{41}^{(2)} + T_{44}^{(1)}T_{44}^{(2)}]$$

$$A_{13} = -T_{31}^{(3)}T_{13}^{(2)} - T_{32}^{(3)}T_{23}^{(2)} - T_{33}^{(3)}T_{33}^{(2)} - T_{34}^{(3)}T_{43}^{(2)}$$

$$A_{21} = T_{41}^{(3)}[T_{13}^{(1)}T_{11}^{(2)} + T_{43}^{(1)}T_{14}^{(2)}] + T_{42}^{(3)}[T_{13}^{(1)}T_{21}^{(2)} + T_{43}^{(1)}T_{24}^{(2)}] + T_{43}^{(3)}[T_{13}^{(1)}T_{31}^{(2)} + T_{43}^{(1)}T_{34}^{(2)}] + T_{44}^{(3)}[T_{13}^{(1)}T_{41}^{(2)} + T_{43}^{(1)}T_{44}^{(2)}]$$

$$A_{22} = T_{41}^{(3)}[T_{14}^{(1)}T_{11}^{(2)} + T_{44}^{(1)}T_{14}^{(2)}] + T_{42}^{(3)}[T_{14}^{(1)}T_{21}^{(2)} + T_{44}^{(1)}T_{24}^{(2)}] + T_{43}^{(3)}[T_{14}^{(1)}T_{31}^{(2)} + T_{44}^{(1)}T_{34}^{(2)}] + T_{44}^{(3)}[T_{14}^{(1)}T_{41}^{(2)} + T_{44}^{(1)}T_{44}^{(2)}]$$

$$A_{23} = -T_{41}^{(3)}T_{13}^{(2)} - T_{42}^{(3)}T_{23}^{(2)} - T_{43}^{(3)}T_{33}^{(2)} - T_{44}^{(3)}T_{43}^{(2)}$$

$$A_{31} = -T_{33}^{(1)}, \quad A_{32} = -T_{34}^{(1)}$$

$$B_{11} = T_{32}^{(3)}[T_{13}^{(1)}T_{31}^{(2)} + T_{43}^{(1)}T_{34}^{(2)}], \quad B_{12} = T_{32}^{(3)}[T_{14}^{(1)}T_{31}^{(2)} + T_{44}^{(1)}T_{34}^{(2)}], \quad B_{13} = -T_{32}^{(3)}T_{33}^{(2)}$$

$$B_{21} = T_{42}^{(3)}[T_{13}^{(1)}T_{31}^{(2)} + T_{43}^{(1)}T_{34}^{(2)}], \quad B_{22} = T_{42}^{(3)}[T_{14}^{(1)}T_{31}^{(2)} + T_{44}^{(1)}T_{34}^{(2)}], \quad B_{23} = -T_{42}^{(3)}T_{33}^{(2)}$$